RobustICA-based Speckle Reduction of PolSAR Images

Chang JIANG [*,1], Jun WANG[1], Yunsong SHI [2], Wenmei LI [1] and Jian GAO[1]

[1]*Geographic Information Department,* Nanjing University of Posts and Communications, Nanjing, Jiangsu,210023, P.R. China

[2]Nanjing University of Chinese Medicine, Nanjing, Jiangsu , 210023, P.R. China

***Abstract* — On the basis of RobustICA, this paper proposes a speckle reduction of PolSAR images by deploying step size polynomials to improve the objective function, obtaining the global optimal step size, and finally exacting the source image estimations with less noise. These experiments were conducted using ESAR data, whose effects were evaluated using the new methods from the coherent speckles index, mean square error, flatness index, the equivalent number of looks and the edge keeping index. The results show that new filter has better denoising effects and edge keeping ability, as well as better time efficiency.**

Keywords- PolSAR; speckle; kurtosis; optimal step size; RobustICA

I. INTRODUCTION

PolSAR images are rich in target information, which are widely used in target detection, and land classification [1, 2]. However, due to the enormous and coherent speckles, the PolSAR images cannot be clearly interpreted, and sometimes cannot be used. Current widespread filtering methods include two main classes: the multilook process during imaging [3] and the speckle reduction after imaging. Multilook is a processing task that averages all the separate images from each subband, which is performed in the frequency domain[4] . The single look PolSAR data are usually multilook-processed to despeckle. However, multilook PolSAR data are suitable for homogeneous areas . [5-7]The former reduces the speckle noise because the multilook process lowers the use of signal bandwidth and sacrifices spatial resolution.The latter includes reduction methods like space domain and frequency domain[8] as well as polarization domain [9]. The boxcar filter is effective when applied to speckle suppression of a homogenous region while reducing the spatial resolution in the heterogenous region [10]. The mininum mean square error (MMSE) filter is the usual method for producing an unbiased estimation of the central pixel value in the selected homogeneous pixels [11]. The refined Lee fitler applies edge-aligned non-squared windows and an MMSE filter to preserve details.Novak and Burl[12] proposed polarimetric whitening filter (PWF) to reduce the speckle of fully polarimetric SAR. However, these methods are time consuming when it comes to maintaining a balance between speckle removal and maintaining both the texture and the edge.

FastICA was proposed by the Finnish scholars Hyvärinen and Oja in 1997 This algorithm converges quickly, and is both easy and convenient because there is no need to manually set parameters, such as adjusting the step size. However, FastICA is not good for a high spatially correlated target signal. Due to this, V. Zarzoso and P. Comon have proposed RobustICA [13]. This algorithm solves the defects in FastICA by separating the spatially correlated signals using a self-adjusting step size polynomial to improve the objective function and choosing the root of the polynomials to obtain the global optimal step size. By comparing the new speckle reduction of PolSAR images on RobustICA, and the reduction using FastICA, this work concludes that the former is not only better at reducing noise but also at improving time efficiency

In this paper, we propose the use of RobustICA to improve time efficiency with despeckling while preserving spatial resolution. The performance of the proposed method is presented and analyzed on the L band ESAR data in the Oberpfaffenhofen area of Germany and comparison with the FastICA. The results demonstrate the performance and availability of the proposed method. The remainder of this work is organized as follows. Section 2 introduces the basic concepts of PolSAR data as the basis of this letter. Section 3 presents the detail of the proposed methodology. In section 4, experiment results based on PolSAR data are shown, and the evaluation indexes are discussed. Finally, we conclude this paper in section 5.

II. THE MODEL AND THE FEATURE OF POLSAR IMAGES

PolSAR measures the scatter echo of each resolution unit in the surface of the earth and obtains the polarized scatter matrix S, which can describe the images' range and phase characteristics, the form of which is as follows:

$$S=\begin{vmatrix} S_{hh} & S_{hv} \\ S_{vh} & S_{vv} \end{vmatrix} \tag{1}$$

In the above, Sij, i represents the status of polarization in the emissions, and j represents the status of polarization in the receiving process, i.e. polarized by the unit i. The matrix vectorization has two approaches: the resolution lexicographic basis and resolution based on the Pauli matrix. The respective forms of vectorization in s are as follows:

$$K_L=\begin{bmatrix} S_{hh} & \sqrt{2}S_{hv} & S_{vv} \end{bmatrix}^T \tag{2}$$

$$K_P = \frac{1}{\sqrt{2}}\left[S_{hh} + S_{vv} \quad S_{hh} - S_{vv} \quad 2S_{hv}\right]^T \tag{3}$$

III. THE BASIC IDEAS OF THE ICA ALGORITHM

A. Classic ICA algorithm ideas

ICA is a process for seeking the optimal solution by optimizing the criteria of certain independence. Hence, ICA includes the principles of the evaluation signal's independence and the maximization of the objective function. The former deploys the objective function for evaluation while the latter deploys an optimizing algorithm. By supposing the variables observed and the independent component variables are both random, and X is the matrix observed while s is the independent component or the sparse code matrix, then the standard ICA hybrid model is as follows:

$$X = AS + T \tag{4}$$

In the above, $X = \{x_1, x_2, x_3, L, x_m\}^T$ indicates the signals observed; A indicates $m \times n$ hybrid matrix, $S = \{s_1, s_2, s_3, \cdots s_n\}^T$ represents the independent component matrix, $s_i \ (i = 1, \cdots, n)$ represents the row vector of independent component matrix. $T = \{t_1, t_2, t_3, \cdots, t_m\}^T$ indicates the noise vector in the Gaussian distribution. The problem lies in the evaluation of the generalized inverse of the hybrid matrix A, i.e. $W = A^+$, in which W is the solution matrix, and the independent component here is:

$$Y = WX \tag{5}$$

In the above equation, $Y = \{y_1, y_2, y_3, \cdots, y_m\}^T$. If y_i remains independent as long as possible, Y can be regarded to be an approximation of S. For the sake of calculation convenience, the signal observed X requires pre-processing before the ICA process.

B. The FastICA Algorithm

Various standard functions together with various optimization methods evolve into various ICA algorithms. Hyvärinen and Oja proposed the FastICA algorithm[14]. This algorithm follows the Newton iteration method to batch process the massive sampling points in the observed data with a fast convergence rate. Kurtosis has been used as the non-Gaussian optimal principle. The definition is as follows:

$$k(y) = E\{y^4\} - 3\left(E\{y^2\}\right)^2 \tag{6}$$

In $y = w^T X$, w^T is the row vector of matrix W. When the kurtosis reaches its maximum value, in $y = w^T X$, the key is to calculate the value of w to make $y = s$. The process of FastICA and the detailed flow is as follows:

Step 1 Make $k = 1$, initialize w and unitize it, which is marked as $w(1)$.

Step 2 Make $w(k) = E\left\{x\left(w(k-1)^T x\right)^3\right\} - 3w(k-1)$, and evaluate $w(\mathrm{k})$ by a certain amount of sampling points.

Step 3 Normalize $w(\mathrm{k})$:

$$w(k) = w(k) / \left\|w(k)\right\| \tag{7}$$

Step 4 If $\left|w(k)\right|$ approximates 1, then output $w(\mathrm{k})$, otherwise return to Step 2.

Step 5 On the basis of $Y = WX$, calculate all the independent components.

Due to the step factor's choice, FastICA gets the cubic convergence rate; meanwhile, the convergence rate at the saddle point and the local extremum lead to a failure in separating signals correctly.

C. RobustICA

RobustICA combines the kurtosis and the gradient optimization based on optimal step technology[13]: first, it transforms the kurtosis function with hybrid signals into a quartic polynomial of the step size.

$$\begin{aligned} k(y) &= \frac{E\{|y|^4\} - 2E^2\{|y|^2\} - \left|E\{y^2\}\right|^2}{E^2\{|y|^2\}} \\ k(\mu) &= \frac{E\{|y^+|^4\} - \left|E\{(y^+)^2\}\right|^2}{E^2\{|y^+|^2\}} - 2 = \frac{P(\mu)}{Q^2(\mu)} - 2 \end{aligned} \tag{8}$$

Where μ is the step size, $Q(\mu) = E\{|y^+|^2\}$ and $y^+ = y + \mu g$, $g = g \cdot x$, $a = y^2$, $b = g^2$, $c = yg$, $d = \mathrm{Re}(yg^*)$, $p(\mu)$ are optimal polynomials, $P(\mu) = E\{|y^+|^4\} - \left|E\{(y^+)^2\}\right|^2$. The root of the polynomial $p(\mu)$ can be calculated algebraically, in which the global optimal step can be picked out to maximize the kurtosis.

$$\mu_{opt} = \arg.\max_{\mu} \left|k(w + \mu g)\right| \tag{9}$$

In the above,

$$g = \nabla_w k(w) \tag{10}$$

Optimization follows the conjugate gradient method. The iterative increment in the conjugate gradient process W is:

$$\nabla_{\mathrm{W}} = \mu \frac{\partial \left| kurt(W \cdot V) \right|}{\partial W} \tag{11}$$

The process of RobustICA and the detailed flow is as follows:

Step 1 Calculate the number N of the source signal, make the number calculator n=1 and presume the number of the source signal is the number of the observed signal;

Step 2 Set the initial value of w as a random normalized vector and make its norm be 1 and its number of iterations $k = 1$.

Step 3 Calculate the parameters of the optimal step polynomials: for the kurtosis comparison function, the parameter can be acquired by $p(\mu) = \sum_{k=0}^{4} a_k \mu^k$, and then find μ_{opt} the max root of the objective function.

Step 4 Refresh the separation matrix $w^+ = w + \mu_{opt} g$, and normalize $w^+ \leftarrow w^+ / \left\| w^+ \right\|$

Step 5 Repeat Step 3 and Step 4 until $\left| w_n(k)^T w_n(k-1) \right|$ is less than 1

Step 6 Orthogonalize $w_n^+ = w_n - WW^T w_n^+$, normalize again , $w_n = w_n / \left\| w_n \right\|$.

Step 7 Make $n = n + 1$, then return to Step 2 to conduct the next iteration until $n = N$, and finally separate.

RobustICA uses the step polynomial, which can be adapted to the parameters to improve the objective function. By choosing the roots of the polynomials, RobustICA gets the global optimal step, which means the value calculated here is the global maximum point and overwhelms the defects of FastICA as separating signals related to space.

IV. EXPERIMENTAL RESULTS

A. Data in this experiment

The data in this experiment came from the ESAR high-resolution single look PolSAR in Germany's Oberpfaffenhofen region. The spatial resolution is 3 m × 3 m, polarized from the L band, from which this experiment chooses a portion with 512 × 512 ,as shown in Figure 1.Figure 2 shows the HH channel intensity image, HV channel intensity image, VH intensity image and VV intensity image.

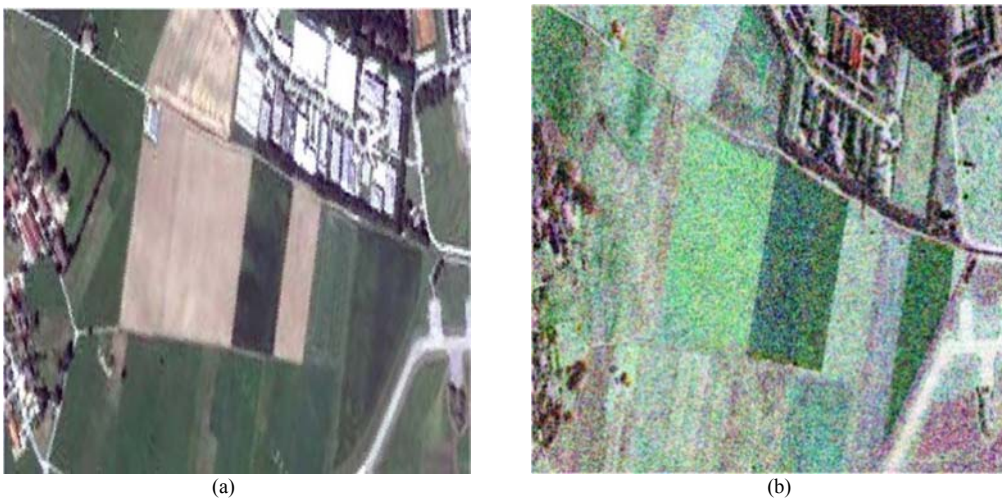

(a) (b)

Figure 1. Image of Oberpfaffenhofen area (512×512)(a) Optical image from Google Map;(b) Pauli decomposition image.

This speckle reduction experiment follows both ICA and RobustICA to test the relative data. ICA separates the speckle noise from the information image on the basis of FastICA. This occurs by changing the polarized intensity image of 512 × 512 into a matrix of 3 × 262,144 composed of a vector of 1 × 262,144. Next, it is important to normalize this matrix, and then centralize and whiten the matrix. Afterward, follow FastICA and RobustICA respectively to separate the noise from the acquired data and evaluate the source signal, transforming it into images sized 512 × 512. In the separation experiment, the image with the lowest speckle index indicates the evaluation of the noise-polluted source image signal while the two remaining independent components indicate the noise. The former seeks to solve the hybrid matrix, while the latter seeks to receive the optimal step algorithm using the kurtosis objective function and accuracy search optimization.

According to this experiment, the two methods respectively obtained two inter-independent images with

speckles and one image with information. The images are shown in Fig. 3. According of Fig. 3 and Fig. 2, the quality of image filtering has been improved and the speckles have been effectively reduced. However, (b) in Fig. 3 has preserved better edge information for the target than (a) and its texture information is clearer.

B. Evaluation index of the filter effect

In order to objectively compare the filtering effects of PolSAR images using FastICA and by RobustICA, this paper chooses the speckle index, the mean variance index, the flatness index, the equivalent number of looks and the edge-preserving coefficient.

1) The coherent speckle index indicates the ratio between the standard deviation and the mean value of the pixel value in the homogeneous region in an image. The smaller the ratio means the pixels have fewer differences, there is less noise, the filtering is better and the speckle reduction is better.

$$\beta=\sqrt{\mathrm{var}(I)}\big/E(I) \tag{12}$$

In the above, E(.) refers to the mean value of the pixel intensity in a homogeneous region; var(.) indicates the variance of pixel intensity in a homogeneous region; I is the original image.

2) The mean square error (MSE) is the mean value of the square sum of the differences before and after the filtering in the homogeneous region in an image. This can evaluate the changes of the image during the course of denoising. The greater the value of MSE, the better the filtering effect is.

$$MSE=\frac{1}{MN}\sum_{i=1}^{M}\sum_{j=1}^{N}\left(I'_{i,j}-I_{i,j}\right)^2 \tag{13}$$

In the above, the area of the image is shown as $M\times N$; I' is the image after filtering, while the remaining signs have the same meaning as those in equation (12).

3) Flatness Index (FI) refers to the filtering's flattening ability to earth polygons. The higher the value is, the better its flattening effect is.

$$FI=M/SD \tag{14}$$

In the above, M and SD respectively indicate the mean value and standard error of all the image elements in various earth polygons after filtering.

4) The edge preserving index refers to the filtering's preservation ability in maintaining the image's vertical and horizontal edges. The closer the ESI value is approximate to 1, the better preserving ability the filtering has.

$$ESI=\frac{\sum_{i=1}^{m}\left|\left(DN_{I'}-DN'_{I'}\right)\right|}{\sum_{i=1}^{m}\left|\left(DN_{I}-DN'_{I}\right)\right|} \tag{15}$$

In the above, DN indicates the pixel value of the images, DN' is the neighbor pixel value of DN.

C. Result

This experiment cut out a homogeneous and heterogeneous region of 49 × 49 pixels and produced three components processed by FastICA and RobustICA, among which the image information has the lowest speckle index. As shown in table 1, when compared with the speckle index of the original image 0.1937, of the three components, the smallest speckle index after FastICA was 0.1229. The smallest index after RobustICA was 0.0973. Regarding separation efficiency, RobustICA took 15.4265 seconds, which was shorter than the time RobustICA took, 54.9249. Regarding the homogeneous region, after comparing the MSE, FI and ENL for component 3 in FastICA and component 1 in RobustICA, we found that RobustICA performed better with filtering effects and flattening ability in various earth polygons, but was weak in speckles after filtering. Regarding the heterogeneous region, after comparing the ESI in the image information component using both algorithms, we found the ESI of component 1 using RobustICA was 0.8615, higher than 0.5286, which was the index for component 3 using FastICA. This illustrates that the former provides better protection for the structure features of PolSAR.

TABLE I Comparison of the Speckle Reduction Index For the Experimental Area

Algorithm	Time-consuming (second)	Component	β
FastICA	54.9249	IC1	0.1482
		IC2	0.1939
		IC3	0.1229
RobustICA	15.4265	IC1	0.0973
		IC2	0.2012
		IC3	0.1063

TABLE II Comparison of speckle reduction index and edge preservation index

Algorithm	Component	MSE	FI	EPI
FastICA	IC1	45.5314	6.7477	0.5296
	IC2	26.6054	5.1580	0.3708
	IC3	46.5672	8.1380	0.5286
RobustICA	IC1	46.7289	10.2770	0.8615
	IC2	46.3599	4.9700	0.2958
	IC3	45.5314	6.7477	0.5296

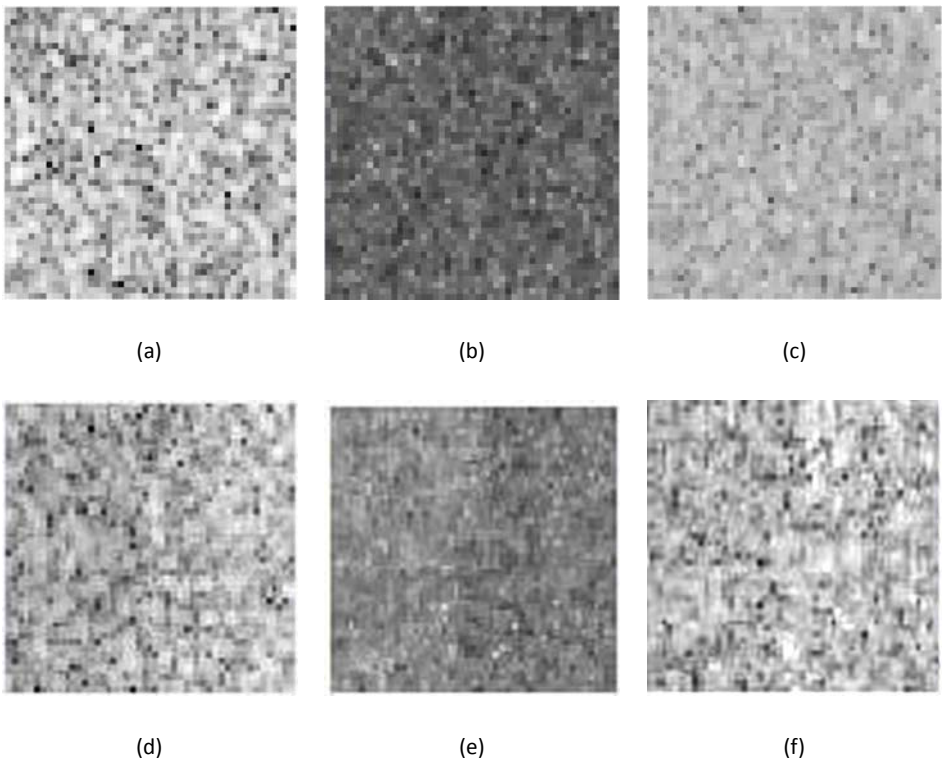

Figure 4. Comparison of filtered results. (a) homogeneous region image; (b) heterogeneous region image; (c) homogeneous region image after FastICA filtering; (d) heterogeneous region image after FastICA filtering ;(e) homogeneous region image after RobustICA filtering;(f) heterogeneous region image after RobustICA filtering

V. CONCLUSIONS

This paper studied the PolSAR image speckle reduction on the basis of RobustICA in blind source separations. First, this study transformed PolSAR images from different channels into vectors, normalized those vectors and then deployed RobustICA to separate the noise in order to select images with the lowest speckle index as objective signals to evaluate. By comparing the results using RobustICA and the results using FastICA, this paper demonstrated that RobustICA, which is used to acquire the optimal step size via accuracy search optimization on the basis of the kurtosis objective function, is not only better at noise reduction but also in improving time efficiency.

ACKNOWLEDGMENTS

This work was financially supported by the National Natural Science Foundation of China (No. 41401480, 41274017) and the Natural Science Foundation of Jiangsu Province (No.BK20130864). Sponsored by NUPTSF (No. NY215181) and Nanjing University of Posts and Telecommunications through Key Bidding Project in Teaching Reform (No. JG03212JX02).The authors would like also to acknowledge the reviewers for their valuable comments.

REFERENCES

[1] M. J. Collins, M. Denbina, and G. Atteia, "On the Reconstruction of Quad-Pol SAR Data From Compact Polarimetry Data For Ocean Target Detection," Ieee Transactions on Geoscience and Remote Sensing, vol. 51, pp. 591-600, Jan 2013.

[2] S. E. Park and W. M. Moon, "Unsupervised classification of scattering mechanisms in polarimetric SAR data using fuzzy logic in entropy and alpha plane," Ieee Transactions on Geoscience and Remote Sensing, vol. 45, pp. 2652-2664, Aug 2007.

[3] J.-S. Lee, A. R. Miller, and K. W. Hoppel, "Statistics of phase difference and product magnitude of multi-look processed Gaussian signals," Waves in Random Media, vol. 4, pp. 307-319, 1994.

[4] B. Liu, Z. H. Zhang, X. Z. Liu, and W. X. Yu, "Edge Extraction for Polarimetric SAR Images Using Degenerate Filter With Weighted Maximum Likelihood Estimation," Ieee Geoscience and Remote Sensing Letters, vol. 11, pp. 2140-2144, Dec 2014.

[5] B. Liu, H. Hu, H. Y. Wang, K. Z. Wang, X. Z. Liu, and W. X. Yu, "Superpixel-Based Classification With an Adaptive Number of Classes for Polarimetric SAR Images," Ieee Transactions on Geoscience and Remote Sensing, vol. 51, pp. 907-924, Feb 2013.

[6] J.-S. Lee, T. L. Ainsworth, Y. Wang, and K.-S. Chen, "Polarimetric SAR Speckle Filtering and the Extended Sigma Filter," Ieee Transactions on Geoscience and Remote Sensing, vol. 53, pp. 1150-1160, Mar 2015.

[7] S. N. Anfinsen, A. P. Doulgeris, and T. Eltoft, "Estimation of the Equivalent Number of Looks in Polarimetric Synthetic Aperture Radar Imagery," Ieee Transactions on Geoscience and Remote Sensing, vol. 47, pp. 3795-3809, Nov 2009.

[8] L. Torres, S. J. S. Sant'Anna, C. D. Freitas, and A. C. Frery, "Speckle reduction in polarimetric SAR imagery with stochastic distances and nonlocal means," Pattern Recognition, vol. 47, pp. 141-157, Jan 2014.

[9] G. Vasile, J.-P. Ovarlez, F. Pascal, and C. Tison, "Coherency Matrix Estimation of Heterogeneous Clutter in High-Resolution Polarimetric SAR Images," Ieee Transactions on Geoscience and Remote Sensing, vol. 48, pp. 1809-1826, Apr 2010.

[10] E. P. Jong-Sen Lee, Polarimetric Radar Imaging: From Basics to Applications, 1st ed. Boca Raton London New York: CRC Press 2009.

[11] S. Goze and A. Lopes, "A MMSE SPECKLE FILTER FOR FULL RESOLUTION SAR POLARIMETRIC DATA," Journal of Electromagnetic Waves and Applications, vol. 7, pp. 717-737, 1993 1993.

[12] L. M. Novak and M. C. Burl, "OPTIMAL SPECKLE REDUCTION IN POLARIMETRIC SAR IMAGERY," Ieee Transactions on Aerospace and Electronic Systems, vol. 26, pp. 293-305, Mar 1990.

[13] V. Zarzoso and P. Comon, "Robust Independent Component Analysis by Iterative Maximization of the Kurtosis Contrast With Algebraic Optimal Step Size," Ieee Transactions on Neural Networks, vol. 21, pp. 248-261, Feb 2010.

[14] A. Hyvarinen and E. Oja, "A fast fixed-point algorithm for independent component analysis," Neural Computation, vol. 9, pp. 1483-1492, Oct 1 1997.